Electromagnetic, Thermal, and Mechanical Modelling of Thin-Wall HTS Bulks During PFM

Santiago Guijosa, Kévin Berger, Frederic Trillaud, Melika Hinaje

Electromagnetic, Thermal, and Mechanical Modelling of Thin-Wall HTS Bulks During PFM

Santiago Guijosa, Kévin Berger, Frederic Trillaud and Melika Hinaje

***Abstract*—High-temperature superconductors, especially rare-earth barium copper oxide (REBCO) bulks, are promising for superseding permanent magnets in power applications. However, being essentially ceramics, their practical use is limited by their brittleness that turns into mechanical failures during high-field magnetization. These failures often arise from defects that appear during the fabrication process, such as pores and cracks. This fragility may be mitigated by including artificial holes in the bulks. The number, size and distributions of these holes may not just improve cooling, but they may also reduce porosity, and enhance both mechanical strength and flux pinning. Modelling the impact of such holes on the trapping performance of the bulks and their thermo-mechanical response to magnetization, particularly the pulsed field magnetization (PFM) that is considered practical for actual applications, is challenging and requires a multiphysics approach. In that context, the present work introduces a 2D finite element model (FEM) that includes coupled electromagnetic, thermal and mechanical physics to simulate thin-wall REBCO bulks with ring reinforcement. The numerical results provide insight on how to maximize trapped magnetic fields while minimizing mechanical loads with thin-wall reinforced REBCO bulks.**

***Index Terms*—Artificial holes, multiphysics finite element analysis, pulsed-field magnetization, REBCO bulk.**

I. Introduction

HIGH-temperature superconducting (HTS) bulks can be used as permanent magnets when magnetized at low temperatures [1], [2]. They can trap magnetic flux density several orders of magnitude higher than conventional magnets for samples weighing less than a few hundreds of grams. A record was broken a few years ago with a trapped field up to 17.6 T achieved between a stack of two bulks [3]. The trapping is generated by the induction of macroscopic superconducting currents in the body of the bulk via the application of a time-dependent external magnetic field. These currents persist in the absence of the external magnetic field. One of the main techniques for field trapping is the Pulsed-field magnetization or PFM [4], [5]. It is the preferred choice for practical applications where bulks can only be magnetized *in situ*, requiring compact setups with a short magnetization process that may last for a few milliseconds. However, due to its duration with rapid flux dynamics, high thermal gradients are generated in the material resulting in a lower intensity of trapped magnetic fields [6], [7]. The same thermal gradient in combination with the Lorentz force lead to the generation of high tensile stresses inside the bulk often leading to fractures. In the worst case scenario, it can result in the loss of its physical integrity [8]–[13].

Rare-earth barium copper oxide (REBCO) bulks are manufactured principally using the top-seeded melt growth (TSMG) method or one of its derivatives [14], [15], such as the top-seeded infiltration growth (TSIG) method and the new single-direction melt growth (SDMG) [16]. The ceramic material is brittle with low tensile strength (≈10-100 MPa). This low strength is attributed to the presence of inherent micro-structural defects such as pores, cracks, and grain boundaries, making them prone to fracture and crack propagation [17]–[20]. Furthermore, porosity (gas trapped in the material) can negatively impact superconducting properties during fabrication as discussed in [21]–[23]. As a result, it could significantly decrease the trapped field and increase tensile stresses during magnetization [24]. Hence, a solution to reduce porosity, and thereby to increase the mechanical resilience and to improve the superconducting properties, is the inclusion of artificial holes. This alternative was proposed in [25]. Thus, prior to the growth process, millimeter-sized holes are drilled in the RE-211 phase, allowing gas to escape the material during the melting process, ultimately reducing porosity and improving superconducting homogeneity through better oxygen annealing. Moreover, holes filled with some thermally conductive and mechanically rigid materials could improve mechanical properties and cooling during magnetization [26], [27]. Such significant improvements in the superconducting, mechanical, and flux-trapping properties, have been found in YBCO materials [25], [28]–[31].

Even though a consequent body of experimental [32]–[36] and numerical [24], [37]–[39] works have been carried out on the magnetization of thin-wall REBCO bulks, there are still some aspects that have not yet been addressed, in particular the electro-thermal-mechanical behavior of such bulks under PFM. In that regard, a 2D finite element multiphysics model built in COMSOL Multiphysics® is proposed hereinafter. The electromagnetic, thermal and mechanical response of a thin-wall REBCO bulk is studied under PFM. The focus is on the use of different materials to fill artificial holes, with and without a metal ring as structural reinforcement to minimize tensile stresses and maximize the trapped field.

II. Modeling framework

In the 2D model illustrated in Fig. 1, the HTS bulk (domain Ω_{sc}) is an infinitely long cylinder encapsulated by an air domain Ω_a, In the present case, the bulk is fastened by a

Version submitted on October 2025. (Corresponding author: Kévin Berger).

Santiago Guijosa, Kévin Berger and Frederic Trillaud are with Université de Lorraine, GREEN, F-54000 Nancy, France (e-mail: santiago.guijosa-gadarrama@univ-lorraine.fr and kevin.berger@univ-lorraine.fr). Frederic Trillaud is also with Instituto de Ingeniería (e-mail: ftrillaudp@ii.unam.mx), Universidad Nacional Autónoma de México, 04510 CDMX, México. Melika Hinaje is with Université de Lorraine, CNRS, LRGP, F-54000, Nancy, France (e-mail: melika.hinaje@univ-lorraine.fr).

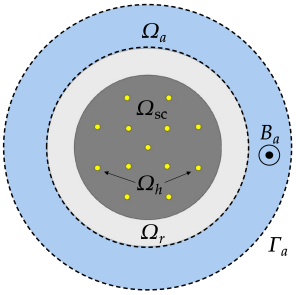

Fig. 1. Definitions of domains and geometry. The YBCO bulk has 13 holes of 1 mm diameter each disposed following a triangular lattice with average separation between holes of 5 mm. Additionally, the model includes a 5 mm thick stainless steel ring for mechanical reinforcement.

TABLE I
CONSTANT MATERIAL PROPERTIES FOR COPPER, SILVER, SN-IN, STYCAST, CU/STYCAST AND YBCO [4], [10], [27], [41], [42].

Property	Copper	Silver	Sn-In	Stycast	Cu/Stycast	YBCO
α_l ($\times 10^{-6}$ K^{-1})	2.7	18.9	10	30	10.9	5
κ (W·m^{-1}·K^{-1})	400	429	50	1.2	280.4	20
E (GPa)	126	83	25	6	90	150
c_p (J·kg^{-1}·K^{-1})	385	235	150	250	345	see [4]
γ_m (kg·m^{-3})	8,940	10,500	7,300	2 400	6,978	5,900
σ_c ($\times 10^6$ S·m^{-1})	60	62	5	0	42	see (2)

stainless steel ring Ω_r (5 mm thickness). The bulk includes 13 holes lumped in the domain Ω_h; each hole is 1 mm in diameter. They are distributed following a triangular lattice, with an average separation between holes of 5 mm. The external pulsed field $B_a(t) = B_m\,(t/\tau)\exp(1-t/\tau)$ is applied along the axial direction at the air boundary Γ_a.

To investigate the effect of different fillers, several commonly used options were selected [27], [28]: copper, silver, Sn–In alloy, Stycast epoxy, and a composite of copper powder mixed with Stycast epoxy. These cases are compared against a reference provided by a bulk without holes, assuming identical superconducting properties for the YBCO material. This simplification was chosen to focus the study on the geometrical impact of the lattice and not the superconducting properties. The properties of the materials, assumed constant in this work, are summarized in Table I. For the Cu/Stycast composite, a 70/30 volume ratio (copper to epoxy) is chosen, and the effective properties are obtained through homogenization. These parameters and properties used in the simulations (see Table II) agree with typical PFM setups and REBCO bulks [28], [40].

A. $\mathbf{H}$-formulation

The electromagnetic model solves the magnetic field $\mathbf{H}$ via,

$$\mu_0 \frac{\partial \mathbf{H}}{\partial t} + \nabla \times (\rho_c \nabla \times \mathbf{H}) = 0, \tag{1}$$

where μ_0 is the permeability of vacuum and ρ_c is the electrical resistivity of the material. The latter is equal to $\rho_c = 1\ \Omega\cdot\mathrm{m}$ for both Ω_a and Ω_h for unfilled holes. For stainless steel and fillers, the resistivity is calculated from the electrical conductivity σ_c given in Table I. The power law model given by (2) is used to describe the resistivity of the superconductor.

$$\rho_{sc} = \frac{E_c}{J_c}\left(\frac{||\mathbf{J}||}{J_c}\right)^{n-1}. \tag{2}$$

E_c is the critical electric field, n is the index of transition, $\mathbf{J}$ is the current density, and J_c is the bulk critical current density which depends on the local magnetic flux density and temperature according to $J_c(\mathbf{B}, T)$ [43]:

$$J_c(\mathbf{B},T) = \frac{J_{c0}}{\left(1+\dfrac{||\mathbf{B}||}{B_0}\right)}\left(1-\left(\frac{T}{T_c}\right)^2\right)^{\frac{3}{2}}. \tag{3}$$

The parameters can be found in Table II.

TABLE II
PARAMETERS FOR THE SIMULATION [4], [40].

Parameter	Description	Value
D	Bulk's diameter	27 mm
D_h	Holes' diameter	1 mm
n_h	Number of holes	13
n	Power law exponent	21
E_c	Electric field criteria	1 μV/cm
J_{c0}	Current density constant	500 A/mm^2
B_0	Flux density constant	1.3 T
B_m	Max. applied field magnitude	4 T
τ	Pulse time constant	13 ms
T_c	Critical temperature	92 K
T_0	Operating temperature	65 K

B. Heat balance equation

Heat is generated in electrically conductive materials via Joule dissipation expressed as $Q = |\mathbf{E}|\cdot|\mathbf{J}|$ to the exception of the "air" and the unfilled holes that are non-conductive by construction. The Joule dissipation Q is a source term in the heat balance equation (4) to solve the temperature across the system made of the HTS, the filled holes and the ring if present.

$$\gamma_m c_p \frac{\partial T}{\partial t} - \nabla\cdot(\kappa\nabla T) = Q. \tag{4}$$

γ_m is the mass density, c_p is the specific heat capacity at constant pressure, and κ is the thermal conductivity of the material. Heat convection, at the exterior of the sample (rim of the bulk or of the stainless steel ring, if present) and at the boundaries of the unfilled holes, is provided by subcooled liquid nitrogen at a constant temperature of 65 K. In the present model, it is mathematically represented by a linearized convective heat flux with a heat transfer coefficient h equal to 600 W·m^{-2}·K^{-1} [44], and no thermal calculations are actually carried out in the domain of the unfilled holes (Ω_h).

C. Mechanical model

Temperature gradients and Lorentz force ($\mathbf{F}_L = \mathbf{J}\times\mathbf{B}$) arise during magnetization thereby deforming the superconductor. The resulting displacement field $\mathbf{u}$ is determined by solving,

$$\nabla\cdot\boldsymbol{\sigma} + \mathbf{F}_L = \gamma_m \frac{\partial^2 \mathbf{u}}{\partial t^2}, \tag{5}$$

TABLE III
COMPARISON OF NUMERICAL RESULTS FOR DIFFERENT FILLERS WITHOUT A REINFORCEMENT RING, SHOWING RELATIVE OR ABSOLUTE CHANGES WITH RESPECT TO THE REFERENCE CASE.

Case	B_t (Δ%)	T_m (Δ%)	σ_{m1} (MPa)	σ_{m2} (Δ%)
Reference	**1.457 T**	**69.5 K**	**0.0**	**2.8 MPa**
Unfilled	−4.962	12.0	4.3	86.1
Copper	−5.665	0.5	0.2	2.8
Silver	−5.759	0.6	0.9	29.2
Sn-In	−5.675	4.6	1.3	57.6
Stycast	−5.533	11.7	4.5	78.5
Cu/Stycast	−5.773	0.8	0.2	20.4

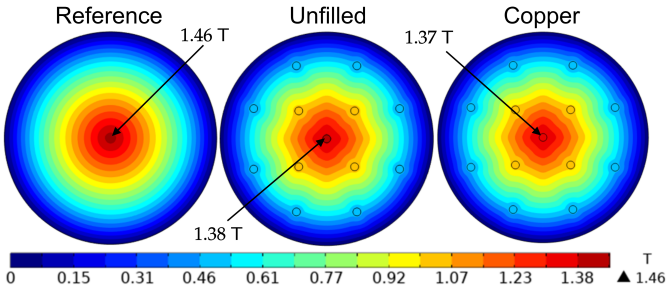

Fig. 2. Magnetic flux density distributions at the end of magnetization (t = 130 s) for: the reference case, the copper fillers, and the unfilled holes, without the stainless steel ring. The thin-wall samples exhibit an inhomogeneous magnetic field distribution, with an approximate 5% reduction in the intensity of the trapped field compared to the reference case.

where $\boldsymbol{\sigma}$ denotes the 2D stress tensor, related to the total strain ε (mechanical and thermal) through the Hooke's law, $\boldsymbol{\sigma} = \mathbf{C}\varepsilon$. $\mathbf{C}$ is the fourth-order stiffness tensor that characterizes the elastic properties of the material. Since ceramics generally fail abruptly when one of the normal stress components exceeds the tensile or fracture strength σ_F, the key mechanical parameter considered in this study is the maximum stress, defined as $\sigma_{\max} = \max(\sigma_r, \sigma_\theta)$ in a 2D cylindrical coordinate system.

III. RESULTS AND DISCUSSION

Table III summarizes the results for the trapped field (B_t), maximum temperature (T_m), and maximum stress (σ_m) during the PFM process for different fillers. These results are compared with the results obtained for the plain reference case (no holes). The trapped field is interpolated at the center of the 2D model. As expected, the introduction of holes leads to a reduction in the trapped field since the same properties for the thin-wall bulk and the ideal reference were assumed. As previously mentioned, different superconducting properties are expected between a reference bulk and a thin-wall sample as a consequence of the fabrication process. In particular, bulks with holes may exhibit improved superconducting properties, such as higher critical current density J_c and critical temperature T_c, due to reduced porosity and enhanced oxygenation. However, to unveil the impact of the geometry and not the change of superconducting properties, a simpler case has been assumed here with equal material properties with and without holes. Thus, within this idealized framework, all thin-wall

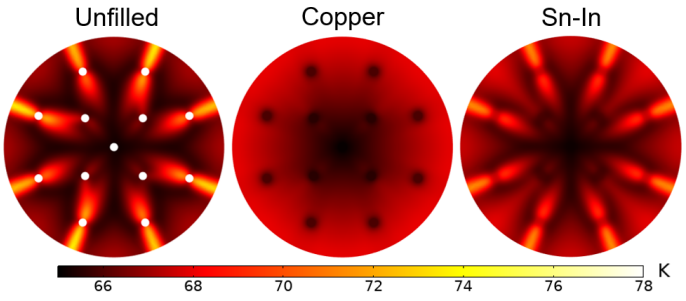

Fig. 3. Comparison of temperature distributions for the unfilled, copper- and Sn-In-filled cases at τ = 13 ms. Poorly conducting or unfilled holes lead to localized temperature hot spots around the holes. Conductive fillers like Copper promote a more homogeneous temperature distribution.

configurations exhibit reductions of comparable magnitude in the trapped magnetic field, with the smallest decrease observed for the unfilled-hole case, which still shows an almost 5% reduction relative to the reference bulk. To evaluate the sensitivity of the results to possible improvements in superconducting performance, an additional simulation was carried out assuming a modest 10% increase in J_c for the thin-wall sample [29], even though studies have found almost a 100% increase [25]. This 10% increase in the J_c leads to an increase of approximately 2% in the trapped magnetic field compared to the reference bulk, partially compensating the geometric reduction. These results indicate that the trapped-field reductions reported here should be interpreted as a lower bound associated with geometry alone.

Figure 2 compares the trapped field distributions for some selected cases: reference, copper, and unfilled. The presence of holes also modifies the magnetic field profile, resulting in a loss of isotropy and cylindrical smoothness with square or hexagon shaped distributions. Besides the differences in magnitude reported in Table III, no significant variations of the field distribution across the bulk are observed between the copper filler and the unfilled case. This non-uniformity is consistent with the expected disturbance of current flow around the holes, which introduces discontinuities in the propagating flux front [38].

The decrease in trapped field with different fillers results from the interplay of several factors like heat diffusion, local variations in the temperature, and inhomogeneous current distributions. Even when enhanced heat diffusion is provided, the average critical current density ($J_c(\mathbf{B}, T)$) can still decrease. Hence, the improved thermal conduction can diffuse the heat across the entire bulk raising everywhere the temperature, in contrast to the unfilled case, where the heat concentrates around the holes resulting in a localized increase in temperature. This can be observed in Fig. 3 with the presence of unfilled or poor thermal conducting fillers that disrupts the homogeneity and isotropy of the temperature distribution across the bulk. Hence, the unfilled-hole and Stycast cases exhibit the highest local temperature rise, with a maximum temperature T_m increase of about 12% compared to the reference case. In contrast, copper- and silver-filled holes with the best thermal conduction reduce the maximum temperature

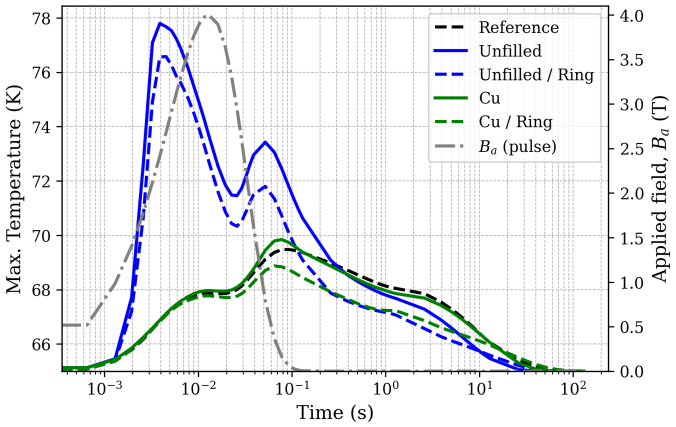

Fig. 4. Comparison of the evolution of the maximum temperature over the HTS bulk during the PFM. The unfilled case exhibits a higher and sharper temperature rise during the pulse ascent due to localized losses around the holes, whereas copper fillers mitigate local heating by enhancing heat diffusion. The use of a metal ring also improves the cooling of the system.

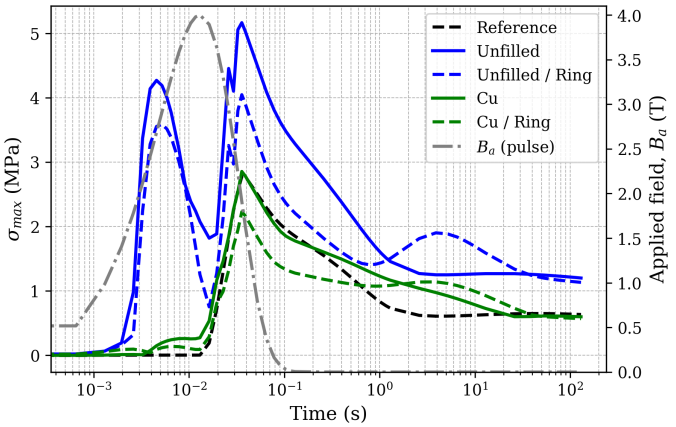

Fig. 5. Comparison of maximum stress evolution during the PFM. Two distinct stress peaks are observed, associated with thermal expansion during the pulse rise and with the Lorentz force during flux trapping. Copper fillers reduce both the magnitude and localization of tensile stresses compared to the unfilled case, as well as the presence of a metal ring.

by spreading the heat evenly around the holes.

Figure 4 compares the evolution of the maximum temperature in the bulk for the copper-filled and unfilled cases. Two contrasting behaviours are observed. The unfilled case has the highest maximum temperature, especially during the ascending stage. The copper fillers not only act as a diffuser of heat but they add mass to the system explaining a lesser maximum temperature rise with fillers than without. In other words, the system has more capacity to absorb energy for a given temperature difference. As an example, the stainless-steel ring when included in the model presents a significant reduction of the maximum temperature even with the unfilled case. Eddy-current heating in the metallic fillers is estimated to be several orders of magnitude lower than that in the bulk and is not included in the model.

Two peaks in maximum tensile stress (σ_{m1} and σ_{m2}) occur during PFM: one is associated with thermal expansion during the pulse rise, and the other is associated with Lorentz force during the flux-trapping stage [24]. The unfilled-hole and Stycast cases show an increase in both peaks (up to 86.1% in σ_{m2}). However, the copper fillers behave as in the reference case with a similar σ_{m1} and an almost negligible 2.8% increase in σ_{m2} compared to other materials. The Cu/Stycast composite exhibits intermediate behavior. It offers better cooling and lower stress than insulating materials but it performs slightly worse than pure copper with a lower thermal conductivity. Fig. 5 compares the evolution of maximum stress for the copper fillers and the unfilled case. The stainless-steel ring fastens the bulk by restraining its expansion during magnetization therefore reducing the tensile stress.

Fig. 6 presents the temperature and stress distributions for the unfilled case. The maximum temperature rise occurs during the pulse ascent, primarily around the holes (Fig. 6(a)), as reported in [24], due to localized losses. This leads to local thermal expansion and the development of tensile stresses as illustrated by Fig. 6(b). During the flux-trapping stage, magnetic flux relocates toward the center of the bulk, producing high electromagnetic tensile stresses. Since there is no mechanical support offered by any filling materials in the holes, stress concentrations set in at the center of the bulk. In contrast, Fig. 7 shows the corresponding distributions for the copper fillers. The temperature rise is mitigated by improved heat diffusion (Fig. 7(a)), preventing the formation of local thermal tensile stresses (see Fig. 7(b). Additionally, the electromagnetic stress during the flux-trapping stage is

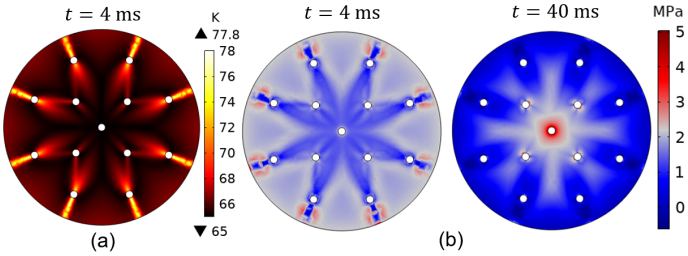

Fig. 6. (a) Temperature distribution at peak temperature ($t \approx 4$ ms). (b) Maximum stress distribution at peak temperature and peak stress ($t \approx 40$ ms) for the unfilled case without the stainless steel ring. Localized heating around the holes during the pulse rise induces thermal expansion and stress concentrations. During flux-trapping stage, the Lorentz force induces tensile stresses in the center of the bulk, amplified by the absence of mechanical support in the holes.

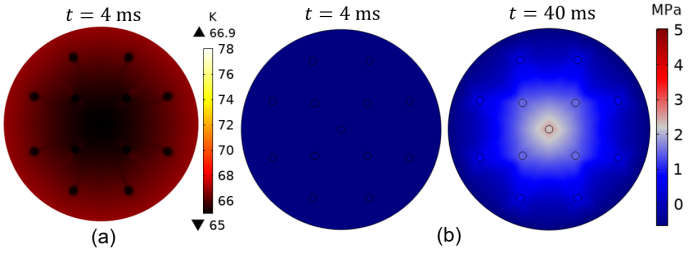

Fig. 7. (a) Temperature distribution at peak temperature ($t \approx 4$ ms). (b) Maximum stress distribution at peak temperature and peak stress ($t \approx 40$ ms) for the copper fillers without the stainless steel ring. For fair comparison, the scale is the same as in the unfilled case. Enhanced heat diffusion provided by copper fillers suppresses local thermal hot spots and promotes a more uniform stress distribution, resulting in reduced peak tensile stresses compared to the unfilled case.

reduced.

To understand the effect of mechanical mismatch [45] introduced by the fillers, a parametric sweep of the filler thermal expansion coefficient α_f and Young's modulus E_f was carried out using values inferior to, equal to, and superior to those of the HTS, namely $\alpha_f = \{1.67,\ 5,\ 15\} \times 10^{-6}\,\mathrm{K}^{-1}$ and $E_f = \{50,\ 150,\ 450\}\,\mathrm{GPa}$. The remaining material properties are those of copper (see Table I). The corresponding normalized mismatch parameters are defined as:

$$M_\alpha = \log\left(\frac{\alpha_f}{\alpha_{\mathrm{HTS}}}\right) = \begin{cases} < 0, & \text{less expansive,} \\ = 0, & \text{equally expansive,} \\ > 0, & \text{more expansive.} \end{cases} \tag{6}$$

$$M_E = \log\left(\frac{E_f}{E_{\mathrm{HTS}}}\right) = \begin{cases} < 0, & \text{softer,} \\ = 0, & \text{matched,} \\ > 0, & \text{stiffer.} \end{cases} \tag{7}$$

These parameters provide a useful centred description of the mechanical mismatch between the filler and the bulk. Fig. 8 summarizes the results of the parameter sweep showing the envelope of possible stresses bounded by a minimum and maximum stress curve. It can be seen that the lower bound corresponds to matching the filler mechanical properties to the bulk ($M_E = M_\alpha = 0$), while the upper bound corresponds to two cases differentiating the properties of the bulk from those of the fillers. All intermediate combinations lie between those two limits. The results are also compiled in Fig. 9 as the increment of each stress peak on top of the matched case. Although present, the initial stress peak σ_{m1} remains almost negligible for all configurations due to the high thermal conductivity of the filler. The dominant contribution are the second peak σ_{m2}, occurring during the Lorentz force driven stage, and a later stress peak σ_{m3} visible on the red curve in Fig. 8.

The increase of σ_{m2} depends primarily on the stiffness mismatch M_E. Even in the absence of thermal expansion mismatch ($M_\alpha = 0$), it increases when $M_E \neq 0$. Both softer fillers ($M_E < 0$) and stiffer fillers ($M_E > 0$) lead to higher σ_{m2} values compared to the matched case. At later times, when the external field is removed and a slight increase in temperature is induced due to the changing currents (see Fig. 4 at $t \approx 10^{-1}$ s), an additional stress peak σ_{m3} emerges when more expansive fillers are introduced. This third peak is smaller for matched or less expansive fillers ($M_\alpha \leq 0$) but it notably increases for a positive mismatch ($M_\alpha > 0$). The magnitude of σ_{m3} is further amplified when combined with stiffness mismatch, indicating that differential expansion between the filler and the bulk becomes an important source of tensile stress.

IV. Conclusions

A 2D multiphysics finite element model was developed to investigate the coupled electromagnetic, thermal, and mechanical behavior of REBCO thin-wall bulks under PFM. The results indicate that the presence of holes reduces the trapped field compared to the ideal reference case (no holes),

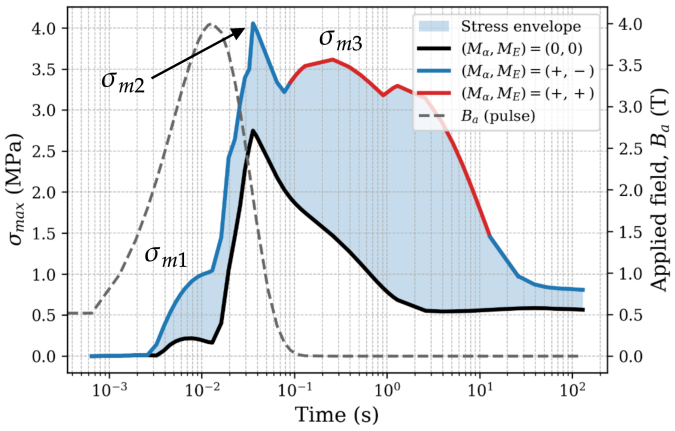

Fig. 8. Maximum tensile stress evolution for different mechanical mismatches, showing a stress envelope bounded by the matched case (minimum) and two representative mismatched cases (maximum).

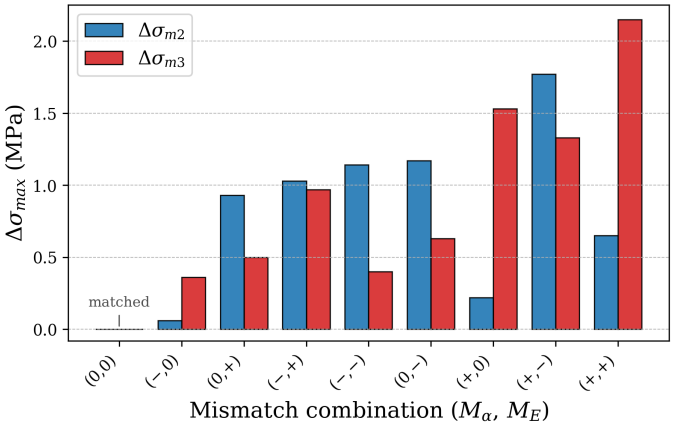

Fig. 9. Increment of stress peaks $\Delta\sigma_{m2}$ and $\Delta\sigma_{m3}$ relative to the matched case $(M_\alpha, M_E) = (0, 0)$, for all mismatch combinations.

assuming identical superconducting properties, although in practice, holes may enhance mechanical and superconducting performance. Therefore, the results should be interpreted as a lower bound related to the geometry alone. Filling the holes with materials combining high thermal conductivity and similar Young's modulus and thermal expansion coefficient to the bulk is essential to limit temperature rise and suppress local tensile stresses. Hence, copper appears as the best choice among the studied materials. Nevertheless, its manufacture might be difficult, making the Cu/Stycast epoxy a practical trade-off. Finally, the addition of a ring reinforcement provides extra cooling and compressive support, reducing tensile stresses.

Acknowledgments

F. Trillaud thanks the Dirección General de Asuntos del Personal Académico of the Universidad Nacional Autónoma de México under Grant DGAPA-PAPIIT 2024 (#IN104124) and the Mexican federal fund, Ciencia básica y de frontera 2023-2024 of the Secretaría de Ciencia, Humanidades, Tecnología e Innovación (SECIHTI), grant CBF2023-2024-2288.

REFERENCES

[1] Q. Wang, H. Zhang, L. Hao, and T. Coombs, "Review on high-temperature superconducting trapped field magnets," *Superconductor Science and Technology*, vol. 37, no. 12, p. 123005, nov 2024. [Online]. Available: https://dx.doi.org/10.1088/1361-6668/ad8bf8

[2] J. R. Hull and M. Murakami, "Applications of bulk high-temperature superconductors," *Proceedings of the IEEE*, vol. 92, no. 10, pp. 1705–1718, 2004.

[3] J. H. Durrell, A. R. Dennis, J. Jaroszynski, M. D. Ainslie, K. G. B. Palmer, Y.-H. Shi, A. M. Campbell, J. Hull, M. Strasik, E. E. Hellstrom, and D. A. Cardwell, "A trapped field of 17.6T in melt-processed, bulk Gd-Ba-Cu-O reinforced with shrink-fit steel," *Superconductor Science and Technology*, vol. 27, no. 8, p. 082001, jun 2014. [Online]. Available: https://dx.doi.org/10.1088/0953-2048/27/8/082001

[4] M. D. Ainslie, H. Fujishiro, H. Mochizuki, K. Takahashi, Y.-H. Shi, D. K. Namburi, J. Zou., D. Zhou, A. R. Dennis, and D. A. .Cardwell, "Enhanced trapped field performance of bulk high-temperature superconductors using split coil, pulsed field magnetization with an iron yoke," *Superconductor Science and Technology*, vol. 29, no. 7, p. 074003, may 2016. [Online]. Available: https://dx.doi.org/10.1088/0953-2048/29/7/074003

[5] M. D. Ainslie, J. Srpcic, D. Zhou, H. Fujishiro, K. Takahashi, D. A. Cardwell, and J. H. Durrell, "Toward optimization of multi-pulse, pulsed field magnetization of bulk high-temperature superconductors," *IEEE Transactions on Applied Superconductivity*, vol. 28, no. 4, pp. 1–7, 2018.

[6] K. Berger, J. Leveque, D. Netter, B. Douine, and A. Rezzoug, "Influence of temperature and/or field dependences of the $e - j$ power law on trapped magnetic field in bulk ybacuo," *IEEE Transactions on Applied Superconductivity*, vol. 17, no. 2, pp. 3028–3031, 2007.

[7] H. Fujishiro and T. Naito, "Simulation of temperature and magnetic field distribution in superconducting bulk during pulsed field magnetization," *Superconductor Science and Technology*, vol. 23, no. 10, p. 105021, sep 2010. [Online]. Available: https://dx.doi.org/10.1088/0953-2048/23/10/105021

[8] Y. Ren, R. Weinstein, J. Liu, R. Sawh, and C. Foster, "Damage caused by magnetic pressure at high trapped field in quasi-permanent magnets composed of melt-textured ybacuo superconductor," *Physica C: Superconductivity*, vol. 251, no. 1, pp. 15–26, 1995. [Online]. Available: https://www.sciencedirect.com/science/article/pii/0921453495003983

[9] X. Yang, X. Li, Y. He, X. Wang, and B. Xu, "Investigation on stresses of superconductors under pulsed magnetic fields based on multiphysics model," *Physica C: Superconductivity and its Applications*, vol. 535, pp. 1–8, 2017. [Online]. Available: https://www.sciencedirect.com/science/article/pii/S0921453416302659

[10] M. D. Ainslie, K. Y. Huang, H. Fujishiro, J. Chaddock, K. Takahashi, S. Namba, D. A. Cardwell, and J. H. Durrell, "Numerical modelling of mechanical stresses in bulk superconductor magnets with and without mechanical reinforcement," *Superconductor Science and Technology*, vol. 32, no. 3, p. 034002, feb 2019. [Online]. Available: https://dx.doi.org/10.1088/1361-6668/aaf851

[11] F. Trillaud, K. Berger, B. Douine, and J. Lévêque, "Distribution of current density, temperature and mechanical deformation in YBCO bulks under Field-Cooling magnetization," *IEEE Transactions on Applied Superconductivity*, vol. 28, no. 4, Jun. 2018. [Online]. Available: https://hal.science/hal-01590668

[12] H. Wu, H. Yong, and Y. Zhou, "Stress analysis in high-temperature superconductors under pulsed field magnetization," *Superconductor Science and Technology*, vol. 31, no. 4, p. 045008, mar 2018. [Online]. Available: https://dx.doi.org/10.1088/1361-6668/aaafaa

[13] K. Takahashi, H. Fujishiro, T. Naito, Y. Yanagi, Y. Itoh, and T. Nakamura, "Fracture behavior analysis of eubacuo superconducting ring bulk reinforced by a stainless steel ring during field-cooled magnetization," *Superconductor Science and Technology*, vol. 30, no. 11, p. 115006, oct 2017. [Online]. Available: https://dx.doi.org/10.1088/1361-6668/aa8827

[14] D. K. Namburi, Y. Shi, and D. A. Cardwell, "The processing and properties of bulk (re)bco high temperature superconductors: current status and future perspectives," *Superconductor Science and Technology*, vol. 34, no. 5, p. 053002, mar 2021. [Online]. Available: https://dx.doi.org/10.1088/1361-6668/abde88

[15] G. Krabbes, G. Fuchs, W. R. Canders, H. M., and R. Palka, *High temperature superconductor bulk materials: fundamentals, processing, properties control, application aspects*. John Wiley & Sons, 2006.

[16] T. Motoki, R. Sasada, T. Tomihisa, M. Miwa, S.-i. Nakamura, and J.-i. Shimoyama, "Development of homogeneous and high-performance rebco bulks with various shapes by the single-direction melt growth (sdmg) method," *Superconductor Science and Technology*, vol. 35, no. 9, p. 094003, jul 2022. [Online]. Available: https://doi.org/10.1088/1361-6668/ac811e

[17] Q. Nouailhetas, Y. Xing, R. Dorget, W. Dirahoui, S. Guijosa, F. Trillaud, J. Lévêque, J. G. Noudem, J. Labbé, and K. Berger, "Characterisation of Large-Sized REBaCuO Bulks for Application in Flux Modulation Machines," *Materials*, vol. 17, no. 15, p. 3827, 2024. [Online]. Available: https://hal.science/hal-04665851

[18] J. V. J. Congreve, Y. Shi, K. Yuan Huang, A. R. Dennis, J. H. Durrell, D. A. Cardwell, "Characterisation of the mechanical failure and fracture mechanisms of single grain y–ba–cu–o bulk superconductors," *Superconductor Science and Technology*, vol. 33, no. 1, p. 015003, dec 2019. [Online]. Available: https://dx.doi.org/10.1088/1361-6668/ab5b46

[19] N. Sakai, A. Mase, H. Ikuta, S.-J. Seo, U. Mizutani, and M. Murakami, "Mechanical properties of sm-ba-cu-o/ag bulk superconductors," *Superconductor Science and Technology*, vol. 13, no. 6, p. 770, jun 2000. [Online]. Available: https://dx.doi.org/10.1088/0953-2048/13/6/328

[20] P. Diko, "Cracking in melt-grown re–ba–cu–o single-grain bulk superconductors," *Superconductor Science and Technology*, vol. 17, no. 11, p. R45, aug 2004. [Online]. Available: https://doi.org/10.1088/0953-2048/17/11/R01

[21] J. V. J. Congreve, Y. H. Shi, A. R. Dennis, J. H. Durrell, and D. A. Cardwell, "Comparison of the superconducting properties of Y-Ba-Cu-O and Y-Ba-Cu-O-Ag bulk superconductors," *IOP Conference Series: Materials Science and Engineering*, vol. 502, no. 1, p. 012181, apr 2019. [Online]. Available: https://dx.doi.org/10.1088/1757-899X/502/1/012181

[22] J. Baumann, Y. Shi, D. Weerakonda, J. H. Durrell, and D. A. Cardwell, "Understanding the porosity and its effects on the superconducting properties of ybco single grains," *Journal of the European Ceramic Society*, vol. 43, no. 4, pp. 1542–1547, 2023. [Online]. Available: https://www.sciencedirect.com/science/article/pii/S0955221922009141

[23] M. Matsui, N. Sakai, S. Nariki, S. J. Seo, and M. Murakami, "Effects of Pt and CeO2 addition on the growth of Nd4Ba2Cu2O10 particles," *Superconductor Science and Technology*, vol. **13**, no. 6, p. 660, jun 2000. [Online]. Available: https://dx.doi.org/10.1088/0953-2048/13/6/306

[24] S. Guijosa, K. Berger, F. Trillaud, V. Rolando Jara-González, and M. Hinaje, "Impact of porosity on the magnitude of trapped magnetic field and mechanical stress in hts bulks during pfm," *Superconductor Science and Technology*, vol. 38, no. 7, p. 075020, jul 2025. [Online]. Available: https://doi.org/10.1088/1361-6668/adedc0

[25] X. Chaud, D. Bourgault, D. Chateigner, P. Diko, L. Porcar, A. Villaume, A. Sulpice, and R. Tournier, "Fabrication and characterization of thin-wall ybco single-domain samples," *Superconductor Science and Technology*, vol. 19, no. 7, p. S590, may 2006. [Online]. Available: https://doi.org/10.1088/0953-2048/19/7/S33

[26] S. Meslin, C. Harnois, C. Chubilleau, D. Horvath, D. Grossin, E. R. Suddhakar, and J. G. Noudem, "Shaping and reinforcement of melt textured yba2cu3o7-δ superconductors," vol. 19, no. 7, p. S585, may 2006. [Online]. Available: https://doi.org/10.1088/0953-2048/19/7/S32

[27] X. Chaud, D. Kenfaui, E. Louradour, and J. G. Noudem, "Thin-wall bulk high temperature superconductor as a permanent cryomagnet," *IEEE Transactions on Applied Superconductivity*, vol. 22, no. 3, pp. 6 800 304–6 800 304, 2012.

[28] K. Y. Huang, T. Hlásek, D. K. N., A. R. Dennis, Y. Shi, M. D. Ainslie, J. V. J. Congreve, V. Plecháček, J. Plecháček, D. A. Cardwell, and J. H. Durrell, "Improved trapped field performance of single grain y-ba-cu-o bulk superconductors containing artificial holes," *Journal of the American Ceramic Society*, vol. 104, no. 12, pp. 6309–6318, 2021. [Online]. Available: https://ceramics.onlinelibrary.wiley.com/doi/abs/10.1111/jace.18017

[29] K. Zmorayová, P. Diko, D. Volochová, V. Antal, T. Hlásek, V. Plecháček, and F. Antončík, "Complex microstructural analysis of ybco single-grain bulks with artificial holes: Effect on superconducting properties," *Ceramics International*, vol. 49, no. 13, pp. 22 177–22 186, 2023. [Online]. Available: https://www.sciencedirect.com/science/article/pii/S027288422300994X

[30] T. Hlásek, K. Y. Huang, J. Esnoz-Larraya, V. Plecháček, J. Durrell, I. Valiente-Blanco, and D. A. Cardwell, "Enhanced mechanical properties of single-domain ybco bulk superconductors processed with artificial holes," *IEEE Transactions on Applied Superconductivity*, vol. 29, no. 5, pp. 1–4, 2019.

[31] S. Haindl, F. Hengstberger, H. W. Weber, S. Meslin, J. Noudem, and X. Chaud, "Hall probe mapping of melt processed superconductors with artificial holes," *Superconductor Science and Technology*, vol. 19, no. 1, p. 108, dec 2005. [Online]. Available: https://doi.org/10.1088/0953-2048/19/1/018

[32] G. P. Lousberg, J.-F. Fagnard, J. G. Noudem, M. Ausloos, B. Vanderheyden, and P. Vanderbemden, "Measurement of the magnetic field inside the holes of a drilled bulk high-tc superconductor," *Superconductor Science and Technology*, vol. 22, no. 4, p. 045009, mar 2009. [Online]. Available: https://doi.org/10.1088/0953-2048/22/4/045009

[33] G. P. Lousberg, J.-F. Fagnard, E. Haanappel, X. Chaud, M. Ausloos, B. Vanderheyden, and P. Vanderbemden, "Pulsed-field magnetization of drilled bulk high-temperature superconductors: flux front propagation in the volume and on the surface," *Superconductor Science and Technology*, vol. 22, no. 12, p. 125026, oct 2009. [Online]. Available: https://doi.org/10.1088/0953-2048/22/12/125026

[34] H. Fujishiro, T. Naito, D. Furuta, and K. Kakehata, "Temperature measurements in small holes drilled in superconducting bulk during pulsed field magnetization," *Physica C: Superconductivity and its Applications*, vol. 470, no. 20, pp. 1181–1184, 2010, proceedings of the 22nd International Symposium on Superconductivity (ISS 2009). [Online]. Available: https://www.sciencedirect.com/science/article/pii/S0921453410003254

[35] H. Fujishiro, S. Kawaguchi, M. Kaneyama, A. Fujiwara, T. Tateiwa, and T. Oka, "Heat propagation analysis in htsc bulks during pulse field magnetization," *Superconductor Science and Technology*, vol. 19, no. 7, p. S540, may 2006. [Online]. Available: https://doi.org/10.1088/0953-2048/19/7/S23

[36] K. Yokoyama, K. Eranda, Y. Zhao, A. Katsuki, A. Miura, and T. Oka, "Influence of artificial defects on trapped field performance in a superconducting bulk magnet," *Journal of Physics: Conference Series*, vol. 871, no. 1, p. 012050, jul 2017. [Online]. Available: https://doi.org/10.1088/1742-6596/871/1/012050

[37] G. Lousberg, M. Ausloos, P. Vanderbemden, and B. Vanderheyden, "Bulk high-Tc superconductors with drilled holes: How to arrange the holes to maximize the trapped magnetic flux?" *Superconductor Science and Technology*, vol. 21, 11 2008.

[38] G. P. Lousberg, J.-F. Fagnard, M. Ausloos, P. Vanderbemden, and B. Vanderheyden, "Modification of the trapped field in bulk high-temperature superconductors as a result of the drilling of a pattern of artificial columnar holes," *Journal of Physics: Conference Series*, vol. 234, no. 1, p. 012023, Jun. 2010.

[39] Y. Ru, H. Yong, and Y. Zhou, "Numerical simulation of dynamic fracture behavior in bulk superconductors with an electromagnetic-thermal model," *Superconductor Science and Technology*, vol. 32, no. 7, p. 074001, may 2019. [Online]. Available: https://dx.doi.org/10.1088/1361-6668/ab0e93

[40] D. K. Namburi, K. Takahashi, T. Hirano, T. Kamada, H. Fujishiro, Y.-H. Shi, D. A. Cardwell, J. H. Durrell, and M. D. Ainslie, "Pulsed-field magnetisation of y-ba-cu-o bulk superconductors fabricated by the infiltration growth technique," *Superconductor Science and Technology*, vol. 33, no. 11, p. 115012, sep 2020. [Online]. Available: https://dx.doi.org/10.1088/1361-6668/abb590

[41] C. Inc., "Comsol multiphysics®," 2024, accessed: 2024-12-04. [Online]. Available: https://www.comsol.com/

[42] L. MatWeb, "Matweb: The online materials information resource," 2025, accessed: 2025-10-10. [Online]. Available: https://www.matweb.com/index.aspx

[43] M. D. Ainslie and H. Fujishiro, *Numerical Modelling of Bulk Superconductor Magnetisation*, ser. 2053-2563. IOP Publishing, 2019. [Online]. Available: https://dx.doi.org/10.1088/978-0-7503-1332-2

[44] M. Yazdani-Asrami, M. Staines, G. Sidorov, and A. Eicher, "Heat transfer and recovery performance enhancement of metal and superconducting tapes under high current pulses for improving fault current-limiting behavior of hts transformers," *Superconductor Science and Technology*, vol. 33, no. 9, p. 095014, aug 2020. [Online]. Available: https://dx.doi.org/10.1088/1361-6668/aba542

[45] *Effect of Microstructure on Toughness and Strength*. John Wiley Sons, Ltd, 2009, ch. 11, pp. 199–225. [Online]. Available: https://onlinelibrary.wiley.com/doi/abs/10.1002/9780470451519.ch11